Journal of Materials and Environmental Science
ISSN : 2028-2508
e-ISSN : 2737-890X
CODEN : JMESCN

J. Mater. Environ. Sci., 2025, Volume 16, Issue 2, Page 371-381

http://www.jmaterenvironsci.com

Electrodeposition of manganese in choline chloride-urea medium

Moutari M.S. [1*], Kindo A [1], Fousséni S. [1], Alassane. S.[1], Moussa B. [1], Giuseppina C. [2], Philippe L. [2]

[1]Laboratoire de Chimie Analytique, de Physique Spatiale et Energétique (L@CAPSE), UFR Sciences et Technologies), Université Norbert ZONGO (UNZ), Avenue Maurice Yaméogo (Rue de l'indépendance), BP 376 Koudougou, Burkina Faso

[2]Laboratory for Physics of Nanomaterials and Energy (LPNE), University of Mons (UMONS), 20 Place du Parc B 7000 Mons, Belgium

**Corresponding author: Moutari Mahamadou Sambo, Email address: mmahamadousambo@mail.com*

Received *23 Nov 2024,*
Revised *19 Feb 2025,*
Accepted *24 Feb 2025*

Citation*: Moutari M.S., Kindo A., Fousséni S., Alassane. S., Moussa B., Giuseppina C., Philippe L. (2025) Electrodeposition of manganese in choline chloride-urea medium, J. Mater. Environ. Sci., 16(2), 371-381*

Abstract: The electrodeposition of manganese was studied on a glassy carbon electrode in a choline chloride-urea medium at 100 °C. The results obtained by cyclic voltammetry highlight the presence of three cathodic peaks at potentials of -1.50 V,-1.56 V and -1.64 V. These peaks respectively corresponding to the deposition of metallic manganese, the formation of hydroxide manganese and oxide manganese. In addition, the voltammogram presents a loop characteristic of a nucleation and growth phenomenon reflecting a slow deposition kinetics controlled by diffusion. The chronoamperometric analysis confirms the deposition of metallic manganese following a three-dimensional (3D) and two-dimensional (2D) nucleation and growth respectively of progressive types. The diffusion coefficient determined using the Cottrell model is 3.50×10^{-7}

Keywords: *Deep eutectic solvents; Nucleation and Growth; Electrodeposition; Manganese;*

1. Introduction

The number of publications focusing on deep eutectic solvents (DES) and their electrochemical properties, for applications in the field of electrodeposition or energy storage, has continued to explode since the 2000s (Abbott *et al.*, 2004). Indeed, unlike aqueous and organic solvents, these solvents are easy to prepare, relatively biodegradable with an attractive cost price and a low ecological footprint (Choi *et al.*, 2011). Deep eutectic solvents were introduced in 2003 by Abbott et al (Abbott *et al.*, 2003) with the choline chloride-urea mixture in a stoichiometric ratio of 1 :2. In 2014, Abbott et al (Smith *et al.*, 2014), generalized SEP as systems formed from a eutectic mixture of Lewis or Bronsted acids and bases. Thus, since then, several authors have used deep eutectic solvents for the electrodeposition of metals such as palladium (Soma *et al.*, 2020), (Lanzinger *et al.*, 2013), (B€ock *et al.*, 2013), (Manolova *et al.*, 2019) ,silver (Rayée *et al.*, 2017), (Sebastián *et al.*, 2013), (Sebastián *et al.*, 2016), copper (Moutari *et al.*, 2023), (Yang *et al.*, 2014), (Xueliang *et al.*, 2016), zinc (Harati *et al.*, 2012), (Bucko *et al.*, 2019), (Vieira *et al.*, 2015), (Abbott *et al.*, 2011), but, very few studies concern the electrodeposition of manganese, which is nevertheless a highly sought-after base metal.

Manganese is a metal commonly used in various technological fields such as metallurgy, chemical industry (Rodier *et al.*, 2016), glass and ceramic industry, and in the pharmaceutical industry (Chalmin *et al.*, 2003). It is also used in the coating of electrochemical capacitors (Stowell *et al.*, 2003), and in corrosion protection (Mraied *et al.*, 2016). For all these reasons, several alloys are formed from manganese. We can cite manganese-tin, manganese-copper, manganese-zinc alloys etc. All these applications make manganese a metal of attention in several research works, hence the growing interest in its electrodeposition or its obtaining by other deposition methods. For this purpose, several authors in the literature have used aqueous or organic solvents which are expensive and less environmentally friendly for the electrodeposition of manganese (Radhi *et al.*, 2010), (Dai *et al.*, 2020), (Yang *et al.*, 2020), (Rojas-Montes *et al.*, 2017), (Eftekhari *et al.*, 2015), (Martinez *et al.*, 2009), (Nessark *et al.*, 2011), (Karastogianni *et al.*, 2016), (Sleightholme *et al.*, 2011), but few have used deep eutectic solvents. The mainly concerns the work of Hartley et al. (Hartley *et al.*, 2014), which reveals through X-ray absorption spectrometry (EXAFS) measurements the formation of complexes of the type $[MnCl_4]^{2-}$ in choline chloride-urea medium. In the same vein, the measurements carried out by Bozzini et al. (Bozzini *et al.*, 2012), have shown that manganese occurs in several oxidized forms in choline chloride-urea medium (Mn(0), Mn(II), Mn(III), Mn(IV)). This diversified presence of manganese in DES media makes its electrodeposition in the elemental form Mn (0) quite complex. Guo et al. (Guo *et al.*, 2020), performed the electrodeposition of Mn (0) on a glassy carbon electrode in a choline chloride-ethylene glycol medium, the characterization by SEM which allowed the observation of a compact deposit on the surface of the substrate. However, a UV-visible measurement highlights the presence of three absorption peaks which would be linked to the presence of three manganese species in the medium.

The present work consists in electrodepositing of Mn (0) on a glassy carbon electrode, in a choline chloride-urea medium. The electrochemical techniques used are cyclic voltammetry and chronoamperometry.

2. Materials and experimental methods

2.1. Reagents and solution preparation

In order to study the electrochemical behavior of manganese, two reagents were used to the preparation of the solvent (ChCl-U). Choline chloride (ChCl) (Alfa Aesar, 98+%) was purified by recrystallization from absolute ethanol (VWR Chemicals, NORMAPUR), filtered and dried under vacuum and urea (U) (VWR Chemicals, NORMAPUR), all mixed in a molar ratio 1:2. The precursor salt $MnCl_2.4H_2O$ (VWR Chemicals, NORMAPUR) was weighed and added directly without prior treatment into the mixture of choline chloride ((CH3)3NCH2CH2OH(Cl)) and urea ((NH2)2CO) (1 :2) at the beginning of the measurements. Then, the entire solid mixture was heated at 100°C for 2 hours under magnetic stirring, in an oil bath until a homogeneous and transparent liquid was obtained by using a hot plate (IKA C-MAG HS7) equipped with a temperature sensor and temperature control device (IKATRO N ETS-D5).

2.2. Experimental methods

Electrochemical experiments were carried out using a three-electrode system connected to an Autolab PGSTAT302N potentiostat (Metrohm). The measuring cell containing the electrolyte is made of glass. Before use, all glassware is cleaned with MilliQ water and dried in an oven. The working electrode is made of glassy carbon (BASi, geometric area = 0.0707 cm^2). It is polished with an alumina suspension (1.0 µm) - water on a porous neoprene mat (Struers), then subjected to two ultrasonic

periods of 5 minutes and rinsed with Milli-Q water to eliminate all tracks of alumina, to finally dried with nitrogen. The counter-electrode is a platinum grid of the order of 3 cm^2 of electrochemically active surface. It is cleaned with a flame using a blowtorch of incandescent flame. A silver wire insulated in a capillary tube containing an electrolyte of a mixture of choline chloride-urea (ChCl-U) in 1:2 was used as a reference electrode. It was rinsed with water and dried with absorbent paper.

3. Results and Discussion

3.1. Potentiodynamic study of manganese electrochemical behavior on a glassy carbon electrode.

The impact of the concentration on the electrochemical behavior of manganese was studied and presented in **Figure 1**. The concentration of 10 and 20 mmolal do not allow the study of the electrochemistry of manganese. For this, we have only represented the cyclic voltammograms at 40,60 and 80 mmolal of $MnCl_2.4H_2O$ in **Figure 1**. We note in general that the electrochemical behavior of Mn (II) in the medium is influenced by a variation of concentration. At the concentration of 40 mmolal, the voltammometric curve presents the cathodic peaks C2 and C3. The concentrations of 60 and 80 mmolal present the same electrochemical characteristics,namely the presence of peaks C1,C2 and C3. As this is a fundamental study, the concentration of 60 mmolal will be retained for the rest of the work.

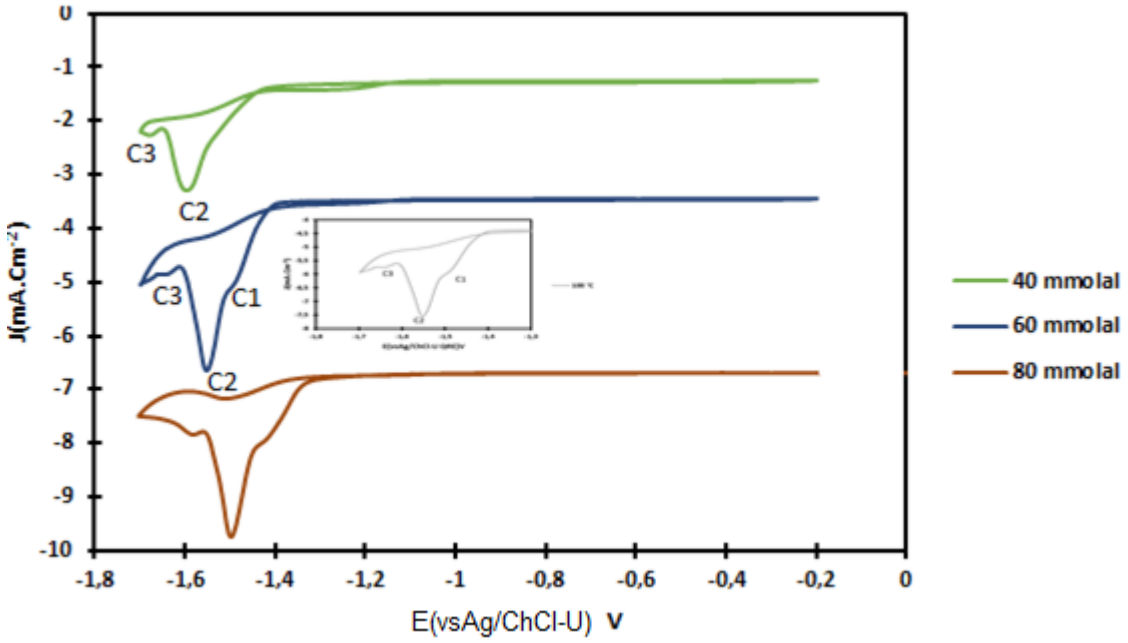

Figure 1: Cyclic voltammograms (3rd cycle) of the ChCl-U system (1 :2), on a glassy carbon electrode, with different concentrations of $MnCl_2.4H_2O$, T=100°C, v=10 $mV.s^{-1}$

Figure 2 shows cyclic voltammograms recorded on a glassy carbon electrode in ChCl-U medium + 60 mmolal of $MnCl_2.4H_2O$ at different temperatures. From a general point of view, it is observed that the shape of the voltammograms obtained is influenced by the variation of the temperature. At the 80°C temperature, an intense peak named peak C2 is observed at the potential of -1.56 V. It is expressly named C2, for a question of consistency with the rest of the analysis at other temperatures because it is preceded by an electrochemical response almost imperceptible at this level of study. This peak C2 corresponds to the formation of the compound $Mn(OH)_2$ following the adsorption of OH^-ions on the surface of Mn (0) (Endres *et al.*, 2017). When the cell temperature is set to 90°C, this leads to the

highlighting of a peak C1 at the potential of -1,50 V, well before the peak C2. It corresponds to the deposition of Mn (0) and this shows in which condition the $Mn(OH)_2$ is formed. Indeed, once the manganese is deposited on the electrode according to **Eqn. 1**, exposure to a solution containing hydroxide ions can lead to the adsorption of these ions on the surface of the manganese. This interaction can lead to the formation of manganese hydroxide according to **Eqn. 2**:

C1: $Mn^{2+} + 2e^- \rightarrow Mn(0)$ **Eqn. 1**

C2: $Mn\ (0)\ +\ 2OH^-(aq) \rightarrow Mn(OH)_2$ **Eqn. 2**

At a temperature of 100°C, a third peak named C3 is highlighted at a potential of -1,64 V. It would correspond to the formation of MnO according to **Eqn. 3**. Beyond the temperature of 100°C, no change in shape is observed. This temperature was therefore chosen for the rest of the measurements.

C3 : $Mn(OH)_2 \rightarrow MnO\ + H_2O$ **Eqn. 3**

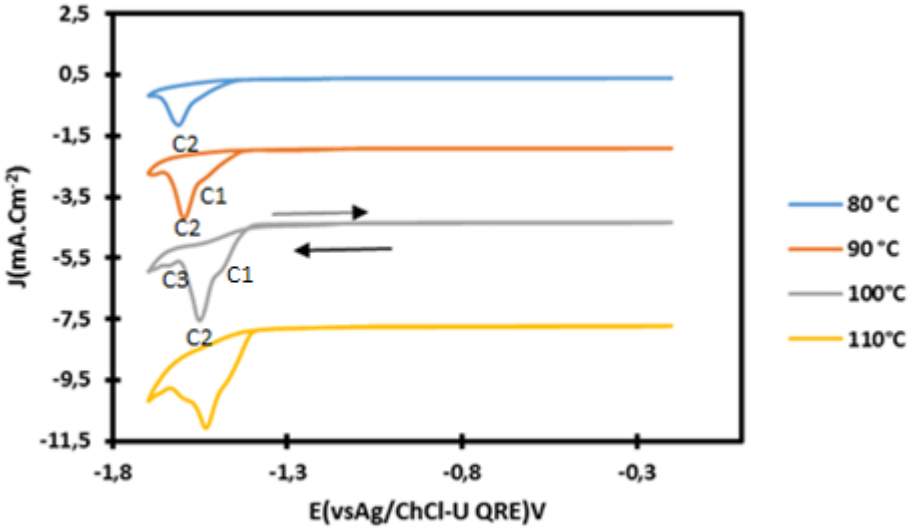

Figure 2 : Cyclic voltammograms (3rd cycle) of ChCl-U + 60 mmolal $MnCl_2.4H_2O$, on a glassy carbon electrode, v=10 $mV.s^{-1}$ at different temperatures.

Its shows by this study that the deposition of Mn (0) on the surface of glassy carbon electrode is influenced by the temperature which promotes the breaking of the O-H bond that exists between hydrogen and oxygen.

Figure 3 examination reveals that the intensity of peak C1 is modified by the rotation speed. This result demonstrates that the deposition of manganese is accompanied by another phenomenon. Namely that of the adsorption of hydroxide ions on the surface of Mn(0). This justifies the presence of a reaction limited by diffusion plates when the rotation speed increases.

To determine the diffusion coefficient of the Mn(II) species,a kinematic viscosity of 0.38 x 10^{-4} $m^2\ s^{-1}$ was calculated based on data from the work of Yadav et al (Yadav *et al.*, 2014), in ChCl-U medium in the temperature range between 293.15 K and 363.15 K. From the Levich slope (box of **figure 3**), a diffusion coefficient equal to 1.79 × 10^{-7} $cm.^2s^{-1}$ was obtained on the glassy carbon electrode. This quantity is in agreement with the value obtained in ChCl-EG medium of 3.53 × 10^{-7}

cm.^{2}s^{-1} at 80°C (Guo *et al.*, 2020), on a glassy carbon electrode and with that of 6.83 × 10^{-8} cm.^{2}s^{-1} obtained in ChCl-U medium at 80°C (Sides *et al.*, 2020), on a platinum electrode.

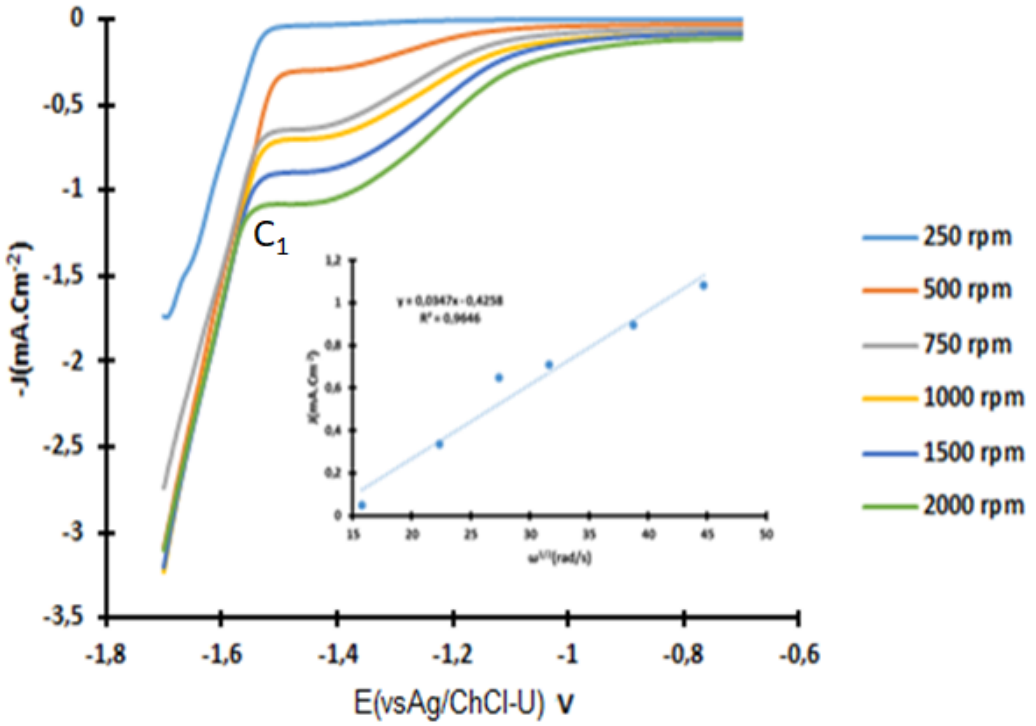

Figure 3: Hydrodynamic voltammograms of the ChCl-U + 60 mmolal $MnCl_2.4H_2O$, system recorded on a rotating carbon disk electrode at different rotation speeds, T=100°C, v=10 mV.s^{-1}.

3.2. Chronoamperometic study of the electrochemical behavior of manganese on a glassy carbon electrode

The transient curves recorded from the system consisting of ChCl-U + 60 mmolal $MnCl_2.4H_2O$ at 100°C on a glassy carbon electrode are present in **Figures 4. To** record these transients, the carbon electrode is subjected to a potential of -0.2V (E1) for 1 s, then to a second potential of -1.28 V (E2) for 5 s, and finally a variable potential E3 is applied for 20 s, from which a current vs.time transient is recorded each time. Generally speaking, the chronoamperometric analysis of the current density transients indicates that they pass through a maximum at short times. At more negative potentials, **Figure 4b** reveals a series of two increasing transitions before reaching the maximum current in absolute values, then a series of two decreasing transitions specifically for the curves recorded by applying the potentials of -1.52 and -1.58 V,whereas they are stable in **Figure 4a**. These series of transitions show that the nucleation and growth of manganese is influenced by other types of reactions attributable to the adsorption/absorption process of hydroxide ions OH^- which constitutes a constraint on the growth of nuclei.

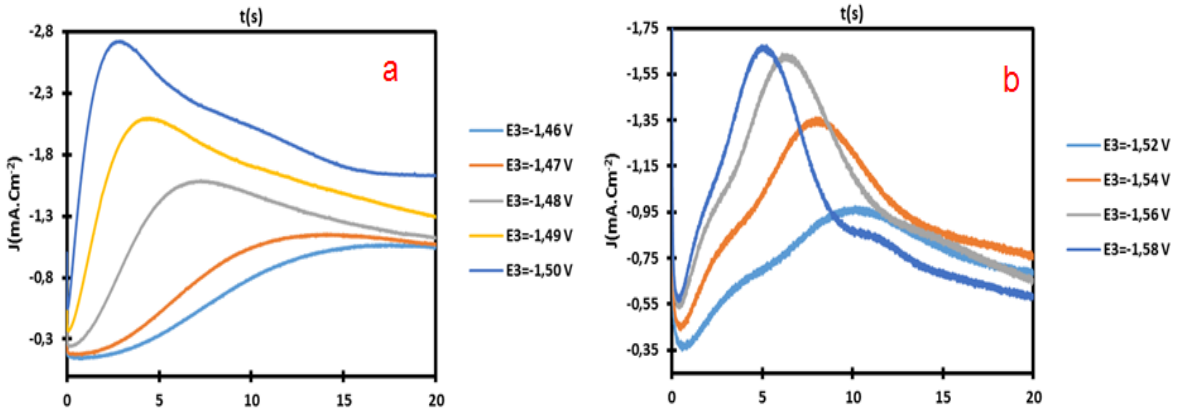

Figure 4: Transients recorded by chronoamperometry in the system ChCl-U (1 :2) + 60 mmolal of $MnCl_2.4H_2O$ on a glassy carbon electrode : (a) E3 between -1.46 V and -1.50V, (b) E3 between -1.52 V and -1.58V, T=100°C.

To better elucidate the mode of nucleation and growth occurring during the electrodeposition of manganese, the dimensionless transient curves were first compared to the theoretical model of Scharifker and Hills. (Scharifker *et al.*, 1983), applied to the three-dimensional nucleation 3D and in a second time to the theoretical model (nucleation and two-dimensional growth 2D) of Bewick and al. (Bewick *et al.*, 1962). However, it should be emphasized that several theoretical models of nucleation and growth are listed in the literature (Scharifker *et al.*, 1983), (Bewick *et al.*, 1962), (Scharifker *et al.*, 1984),(Sluyters-Rehbach *et al.*, 1987). However only the theoretical models of Scharifker and Hills and Bewick and al, were used in this work to account for the observed nucleation and growth phenomena.

The plot of the dimensionless experimental curves of current density $(\frac{j}{j_m})^2$ as a function of $(\frac{t}{t_m})$ obtained by the exploitation of the transients of **Figures 4a** and **4b**. These experimental curves are represented in the same graph as the theoretical curves of Scharifker and Hills (3D) and Hills and Bewick (2D), relating respectively to the instantaneous 3D three-dimensional nucleation and growth **Eqn. 4** and the progressive 3D **Eqn. 5**, the instantaneous 2D two-dimensional nucleation **Eqn. 6** and the progressive 2D **Eqn. 7**:

$$\left(\frac{j}{j_m}\right)^2 = 1.9542 * \left(\frac{t_m}{t}\right) * \left\{1 - \exp\left[-1{,}2564 * \left(\frac{t}{t_m}\right)\right]\right\}^2 \qquad \text{NI } \mathbf{Eqn.\ 4}$$

$$\left(\frac{j}{j_m}\right)^2 = 1.2254 * \left(\frac{t_m}{t}\right) * \left\{1 - \exp\left[-2{,}3367 * \left(\frac{t}{t_m}\right)^2\right]\right\}^2 \qquad \text{NP } \mathbf{Eqn.\ 5}$$

$$\left(\frac{j}{j_m}\right) = \left(\frac{t}{tm}\right) \exp\left\{-\frac{1}{2} * \left(\frac{t^2 - tm^2}{t_m^2}\right)\right\} \qquad \text{NI } \mathbf{Eqn.\ 6}$$

$$\left(\frac{j}{j_m}\right) = \left(\frac{t}{tm}\right)^2 \exp\left\{-\frac{2}{3} * \left(\frac{t^3 - tm^3}{t_m^3}\right)\right\} \qquad \text{NP } \mathbf{Eqn.\ 7}$$

The analysis of Figures 5a and 5b below shows that the shapes of the experimental curves follow respectively the theoretical model of Scharifker and Hills relating to the progressive three-dimensional (3D) nucleation and growth, which would be the consequence of the deposition of the metal on the surface of the electrode and that of Bewick and al relating to the progressive two- dimensional (2D)

nucleation and growth, which would be linked to the adsorption of hydroxide ions on the surface of Mn (II) to give the compound $Mn(OH)_2$.

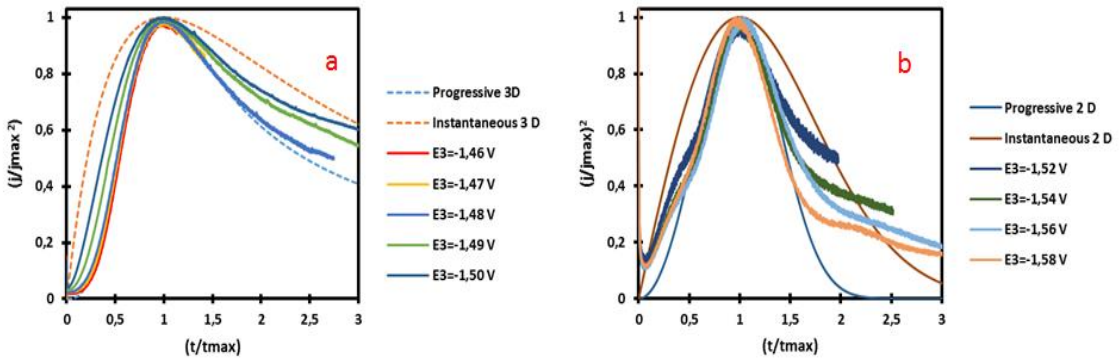

Figure 5: Dimensionless curve $(\frac{j}{j_m})^2 = f(\frac{t}{t_m})$ from current density transients recorded in 60 mmolal of $MnCl_2.4H_2O$+ ChCl-U, T=100°C.

3.3. Characterization of manganese deposition

SEM analysis coupled with EDS surface was undertaken to confirm the effective presence of manganese in accordance with our previous hypotheses. The EDS image in **Figure 6** shows carbon, oxygen, chlorine, aluminum, fluorine, titanium and manganese. Carbon would be bound to the glassy carbon electrode used. Oxygen, nitrogen and chlorine are the constituent elements of the electrolyte. Aluminum would be bound to the residue of the alumina suspension used to polish the electrode surface. Manganese would be related to the deposition of the metal on the surface of the electrode.

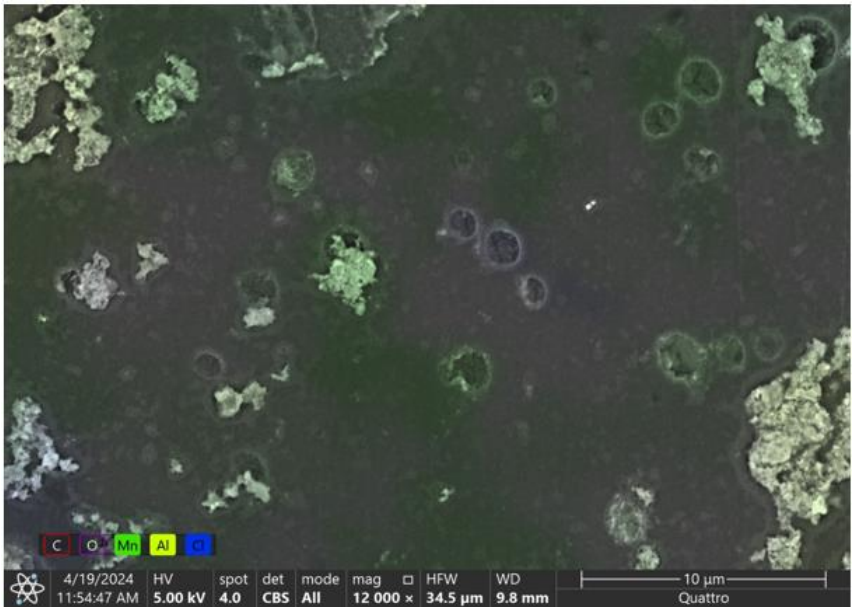

Figure 6: EDS obtained after analysis of the SEM deposit of the sample.

Figure 7 shows the UV-visible absorption spectra recorded at 100°C in the ChCl-U medium**.** The result of the measurements in the orange mixture of $MnCl_2.4H_2O$ allows to highlight two absorption peaks at the wavelength of 264 et 311 nm which would be attributed to the presence of the manganese chloride

complex $[MnCl_4]^{2-}$ and $[Mn(OH)_2Cl_4]^{2-}$ resulting from the adsorption of OH^- ions from the reduction of water molecules contained in the solvent.

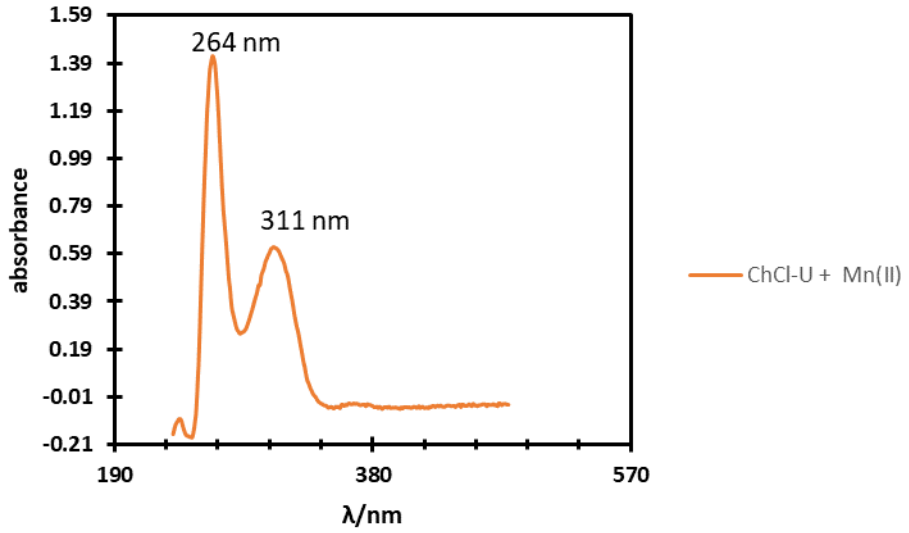

Figure 7: UV-visible spectrum of the salt $MnCl_2.4H_2O$, 60 mmolal in ChCl-U medium.

Conclusion

The present work consisted in electrodepositing manganese in choline chloride-urea medium. The electrochemical results show that parameters such as temperature and rotation speed play a fundamental role in the deposition of manganese in choline chloride-urea medium. However, temperature of 100°C would be optimal for the deposition of metallic manganese and that the speed positively influences the deposition of Mn (0).

The potential of -1.50 V allows a better deposition of Mn(0). The confirmation of the presence of manganese is made by coupling the SEM deposit with surface EDS. The UV-visible characterization highlights the presence of two species of manganese which are $[MnCl_4]^{2-}$ and $[Mn(OH)_2Cl_4]^{2-}$. This work which explored the electrochemical deposition of manganese is continued by our work team in order to find other ways to prevent the formation of compounds ($Mn(OH)_2$ and MnO) which negatively impacts the deposition of Mn (0).

Disclosure statement: *Conflict of Interest:* The authors declare that there are no conflicts of interest.
Compliance with Ethical Standards: This article does not contain any studies involving human or animal subjects.

References

Abbott A.P., Boothby D., Capper G., Davies D.L., et Rasheed R.K. (2004), "Deep Eutectic Solvents Formed between Choline Chloride and Carboxylic Acids: Versatile Alternatives to Ionic Liquids, *Journal of the American Chemical Society*, 126,9142–9147.

Choi Y. H., van Spronsen J., Dai Y., Verberme. M, (2011), "Are Natural Deep Eutectic Solvents the Missing Link in Understanding Cellular Metabolism and Physiology?" *Plant Physiol*., 4, 1701–1705.

Abbott A. P., Capper G., Davies D. L., Rasheed R. K., et Tambyrajah V., (2003) « Novel solvent properties of choline chloride/urea mixtures », *Chem. Commun.*, 1,70-71, doi: 10.1039/b2a10714g.

Smith L., Abbott A. P., et Ryder K. S. (2014) « Deep eutectic solvents (DESs) and their applications », *Chem. Rev*, 21, 11060-11082 doi: 10.1021/cr300162p.

Soma F., Rayée Q., Bougouma M., Baustert C., Buess-Herman C., Doneux T., (2020), Palladium electrochemistry in the choline chloride-urea deep eutectic solvent at gold and glassy carbon electrodes, *Electrochimica Acta 345* ,136165.

Lanzinger G., B€ock R., Freudenberger R., Mehner T., Scharf I., Lampke T., (2013), Electrodeposition of palladium films from ionic liquid (IL) and deep eutectic solutions (DES): physicalechemical characterisation of non-aqueous electrolytes and surface morphology of palladium deposits, *Trans. IMF*.,91,133-140, https://doi.org/10.1179/0020296713Z.00000000097.

B€ock R., Lanzinger G., Freudenberger R., Mehner T., Nickel D., Scharf I., Lampke T., (2013), Effect of additive and current mode on surface morphology of palladium films from a non-aqueous deep eutectic solution (DES), *J. Appl. Electrochem*, 43, 1207-1216, https://doi.org/10.1007/s10800-013-0608-4.

Manolova M., B€ock R. (2019), Electrodeposition of Pd from a deep eutectic solvent system: effect of additives and hydrodynamic conditions, *Trans. Inst. Met.Finish*, 97,161-168, https://doi.org/10.1080/00202967.2019.1605755.

Rayée Q., Doneux T., Buess-Herman C. (2017) Underpotential deposition of silver on gold from deep eutectic electrolytes, *Electrochimica Acta*,237, 127–132.

Sebastián P., Vallés E., Gómez E. (2013), First stages of silver electrodeposition in a deep eutectic solvent. Comparative behavior in aqueous medium, *Electrochim. Acta*, 112, 149–158, http://dx.doi.org/10.1016/j. electacta.2013.08.144.

Sebastián P., Botello L.E., Vallés E., Gómez E., Palomar-Pardavé M., Scharifker B.R., Mostany J. (2016) Three-dimensional nucleation with diffusion controlled growth: A comparative study of electrochemical phase formation from aqueous and deep eutectic solvents, *J. Electroanal. Chem*., http://dx. doi.org/10.1016/j.jelechem.2016.12.014.

Sebastián P., Torralba E., Vallés E., Molina A., Gómez E., (2015), Advances in Copper Electrodeposition in Chloride Excess. A Theoretical and Experimental Approach, *Electrochimica Acta*, 164, 187-195. http://doi.org/10.1016/j.electacta.2015.02.206.

Obeten M. E., Ugi B. U., Alobi N. O., (2017), A review on electrochemical properties of choline chloride based eutectic solvent in mineral processing, *J. Appl. Sci. Environ. Manage*,21 991-998. https://doi.org/10.104314/jasem.v21i5.29.

Bernasconi R., Zebarjadi M., Magagnin L. (2015) Copper electrodeposition from a chloride free deep eutectic solvent, *J. Electroanal. Chem*, 758,163-169. https://doi.org/10.1016/j.jelechem.2015.10.024.

Moutari M. S., Adama K., Bougouma M., Soma F., Sorgho A., Conti Gi, Leclere P., (2023), Temperature effect on zinc electrodeposition in choline chloride-urea deep eutectic solvent, *Mediterranean Journal of Chemistry*, , 13, 228-239, DOI: http://dx.doi.org/10.13171/mjc02306161653bougouma.

Yang H**.**, Reddy R.G., (2014), Electrochemical deposition of zinc from zinc oxide in 2 :1 urea/choline chloride ionic liquid, *Electrochim. Acta*, 147, 513–519.

Xueliang X., Xingli Z.; Xionggang L.; Changyuan L.; Hongwei C.; Qian X.; Zhongfu Z. (2016), Electrodeposition of Zn and CuZn alloy from ZnO/CuO precursors in deep eutectic solvent, *Applied Surface Science, 385*, 481-489, https://doi.org/10.1016/j.apsusc.

Harati M., Love D., Lau W. M., Ding Z., (2012) Preparation of crystalline zinc oxide films by one-step electrodeposition in Reline, *Materials Letters*, 89 339–342.

Bucko M., Tomic M. V., Maksimovic M., Bajat J. B., (2019), The importance of using hydrogen evolution inhibitor during the Zn and Zn-Mn electrodeposition from ethaline, *J. Serb.Chem. Soc.*, 84, 1221-1234.

Vieira L., Schennach R., Gollas B. (2015) The Effect of the Electrode Material on the Electrodeposition of Zinc from Deep Eutectic Solvents, *Electrochimica Acta*, Http://Dx.Doi.Org/10.1016/j.Electacta.2015.11.030**.**

Abbott A.P., Barron J. C., Frisch G., Gurman S., Ryder K. S. et Silva A., (2011), Double Layer Effects on Metal Nucleation in Deep Eutectic Solvents, *Phys. Chem*, 13, 10224–10231.

Rodier J., Legube B., Merlet N., Brunet J., (2009), *l'analyse de l'eau*, 9 e édition, Dunod, Editeur Duno 2016 ISBN: 2100756788, 9782100756780, Longueur :1600 pages.

Chalmin E.; Menu M., Vignaud C., (2003), Analysis of rock art painting and technology of palaeolithic painters, *Measurement Science and Technology*,14, 1590-1597.

Stowell C.A., Wiacek R.J., Saunders A.E., Korgel B.A., (2003), Synthesis and characterization of dilute magnetic semiconductor manganese-doped indium arsenide nanocrystals, Synthesis and Characterization of Dilute Magnetic Semiconductor Manganese-Doped Indium Arsenide Nanocrystals, *Nano Lett*, 3 DOI:10.1021/nl034419+.

Mraied H., Cai W.J., Sagü_es A.A. (2016), Corrosion resistance of Al and Al-Mn thin films, *Thin Solid Films*, 615, https://doi.org/10.1016/j.tsf.2016.07.057.

Radhi M. M., Tan W. T., Ab Rahman M. Z. B, et Kassim A. B. (2010) Electrochemical Reduction of Mn (II) Mediated by C_{60}/Li^+ Modified Glassy Carbon Electrode, *Int. J. Electrochem. Sci*,5, 254 – 266.

Dai X., Zhang M., Li J., Yang D., (2020), Effects of electrodeposition time on a manganese dioxide supercapacitor, *The Royal Society of Chemistry*.

Yang F., Jiang L., Yu X., Lai Y., Li J., (2020), The effects of SeO_2 additive on Mn electrodeposition on Al substrate in MnSO4-$(NH4)_2SO_4$-H_2O solution, *Hydrometallurgy, 192 ,105285.*

Rojas-Montes J.C., Pérez-Garibay R., Uribe-Salas A., Bello-Teodoro S., (2017), Selenium reaction mechanism in manganese electrodeposition process, *Journal of Electroanalytical Chemistry*, 803, 65–71.

Eftekhari A., Molaei F., (2015) carbon nanotube-assisted electrodeposition. Part I: Battery performance of manganese oxide films electrodeposited at low current densities, *Journal of Power Sources*, 274, 1306-1314.

Martinez M. T., Lima A. S., Bocchi N., Teixeira M. F.S. (2009) Voltammetric performance and application of a sensor for sodium ions constructed with layered birnessite-type manganese oxide, *Talanta*,80, 519–525.

Nessark A. B., Habelhames F., Julien C. M., (2011), Preparation and characterization of polybithiophene/β-MnO2 composite electrode for oxygen reduction, *Springer Ionics*, 17, 239–246. DOI 10.1007/s11581-010-0501-7.

Karastogianni S.et. Girousi S. (2016), Electrochemical Behavior and Voltammetric Determination of a Manganese (II) Complex at a Carbon Paste Electrode, *Analytical Chemistry Insights*.

Sleightholme A. E.S., Shinkle A. A., Liua Q., Li Y., Monroe C. W., Thompson L. T. (2011) Non-aqueous manganese acetylacetonate electrolyte for redox flow batteries, *Journal of Power Sources*, 196, 5742–5745.

Hartley J. M., Chung-Man Ip, Forrest G. C. H., Singh K., Gurman S. J., Ryder K. S., Abbott A.P., et G. Frisch, (2014), EXAFS Study into the Speciation of Metal Salts Dissolved in Ionic Liquids and Deep Eutectic Solvents, *Inorg. Chem*, 2014,53, 6280. doi.org/10.1021/ic500824r.

Bozzini B., Gianoncelli A., kaulich B., Mele Cl., Prasciolu M., Kiskinova M., (2012), Electrodeposition of manganese oxide from eutectic urea/choline chloride ionic liquid : An in situ study based on soft X-ray spectromicroscopy and visible reflectivity, *Journal of Power Sources*, 211, 71-76.

Guo M.W., Sun C.B., Yang W.Q., Chen L., Lei H., Zhang Q.B. (2020), Sulphur-induced electrochemical synthesis of manganese nanoflakes from choline chloride/ethylene glycol-based deep eutectic solvent, *Electrochimica Acta*, 341, 136017.

Endres F., Abbott A., et MacFarlane D., (2017), Electrodeposition from ionic liquids, Second. Weinheim, John Wiley & Sons.

Yadav A. et Pandey S., (2014) « Densities and viscosities of (choline chloride + urea) deep eutectic solvent and its aqueous mixtures in the temperature range 293.15 K to 363.15 K », *J. Chem. Eng. Data*, 2221-2229.

Sides W. D., Huang Q. (2018), Electrodeposition of Manganese Thin Films on a Rotating Disk Electrode from Choline Chloride/Urea Based Ionic Liquids, *Electrochim. Acta*, 266, 185–192.

Scharifker B. et Hills G., (1983). Theoretical and experimental studies of multiple nucleation. *Electrochimica Acta*, 28**,** 879–889.

Bewick A., Fleischmann M., Thirsk H.R.**,** (1962), Kinetics of the electrocrystallization of thin films of calomel, *Trans. Faraday Soc*, 58, 2200–2216**.** https://doi.org/10.1039/tf9625802200.

Scharifker B**.**, Mostany J.**,** (1984), Three-dimensional nucleation with diffusion controlled growth. *J. Electroanal. Chem. Interfacial Electrochem*, 177**,** 13–23.

Sluyters-Rehbach M**.**, Wijenberg J.H., Bosco E., Sluyters J.; (1987), The theory of chronoamperometry for the investigation of electrocrystallisation mathematical description and analysis in the case of diffusion-controlled growth. *J. Electroanal. Chem*, 236**,** 1–20.